The EMBO Journal (2004) 23, 450–459 | © 2004 European Molecular Biology Organization | All Rights Reserved 0261-4189/04
www.embojournal.org

THE EMBO JOURNAL

Hematopoietic, angiogenic and eye defects in *Meis1* mutant animals

Tomoyuki Hisa[1,5], Sally E Spence[1,5], Rivka A Rachel[1], Masami Fujita[1,6], Takuro Nakamura[2], Jerrold M Ward[3], Deborah E Devor-Henneman[3], Yuriko Saiki[2], Haruo Kutsuna[4], Lino Tessarollo[1], Nancy A Jenkins[1] and Neal G Copeland[1,*]

[1]Center for Cancer Research, Mouse Cancer Genetics Program, National Cancer Institute, Frederick, MD, USA, [2]The Cancer Institute, Japanese Foundation for Cancer Research, Tokyo, Japan, [3]Center for Cancer Research, Veterinary and Tumor Pathology Section, National Cancer Institute, Frederick, MD, USA and [4]Department of Hematology, Osaka City University Medical School, Osaka, Japan

***Meis1* and *Hoxa9* expression is upregulated by retroviral integration in murine myeloid leukemias and in human leukemias carrying *MLL* translocations. Both genes also cooperate to induce leukemia in a mouse leukemia acceleration assay, which can be explained, in part, by their physical interaction with each other as well as the PBX family of homeodomain proteins. Here we show that *Meis1*-deficient embryos have partially duplicated retinas and smaller lenses than normal. They also fail to produce megakaryocytes, display extensive hemorrhaging, and die by embryonic day 14.5. In addition, *Meis1*-deficient embryos lack well-formed capillaries, although larger blood vessels are normal. Definitive myeloerythroid lineages are present in the mutant embryos, but the total numbers of colony-forming cells are dramatically reduced. Mutant fetal liver cells also fail to radioprotect lethally irradiated animals and they compete poorly in repopulation assays even though they can repopulate all hematopoietic lineages. These and other studies showing that *Meis1* is expressed at high levels in hematopoietic stem cells (HSCs) suggest that *Meis1* may also be required for the proliferation/self-renewal of the HSC.**

The EMBO Journal (2004) **23** 450–459. doi:10.1038/sj.emboj.7600038; Published online 8 January 2004
Subject Categories: development
Keywords: angiogenesis; eye development; hematopoiesis; *Meis1*

Introduction

Meis1 expression is upregulated by retroviral integration in ~15% of BXH2 myeloid leukemias (Moskow *et al*, 1995; Nakamura *et al*, 1996c). *Meis1* encodes a member of the three amino acid loop extension (TALE) family of homeodomain-containing proteins. Within the homeodomain, MEIS1 is most closely related to the PBX family of homeodomain proteins. The founding member of this family, *PBX1*, was identified as the fusion partner of *TCF3* (*E2A*) in human pre-B-cell leukemias carrying a t(1;19)(q23;p13.3) translocation (Kamps *et al*, 1990; Nourse *et al*, 1990). Three additional PBX1-related genes have since been identified (Monica *et al*, 1991; Wagner *et al*, 2001), as have three other *Meis1*-related genes (Nakamura *et al*, 1996a; Berthelsen *et al*, 1998). Most leukemias with retroviral integrations at *Meis1* also have retroviral integrations upstream of *Hoxa7* or *Hoxa9* (Nakamura *et al*, 1996c), with concomitant activation of *Hoxa7* or *Hoxa9* expression. This striking selection for integration and activation of *Meis1* in concert with *Hoxa7*/*Hoxa9* strongly suggests that these genes cooperate to induce leukemia. Additional evidence for cooperation has been provided by Sauvageau and colleagues (Kroon *et al*, 1998), who showed that mouse bone marrow cells engineered to overexpress *Meis1* and *Hoxa9* induce growth factor-dependent oligoclonal acute myeloid leukemia (AML) at <3 months when transplanted into syngenic mice. In contrast, *Meis1* overexpression failed to transform these cells alone, while *Hoxa9* overexpression induced AML but with a longer latency period (Thorsteinsdottir *et al*, 2001).

In humans, *HOXA9* is fused to *NUP98* in AMLs carrying a t(7;11)(p15;p15) translocation (Borrow *et al*, 1996; Nakamura *et al*, 1996b). *MEIS1* and *HOXA9* are also frequently coexpressed in human AMLs (Lawrence *et al*, 1999; Afonja *et al*, 2000) and are upregulated in acute lymphocytic leukemias carrying *MLL* translocations (Rozovskaia *et al*, 2001). *MEIS1* may therefore also be a human leukemia disease gene.

The affinity and specificity of DNA binding by HOX proteins is augmented by their interaction with PBX. *In vitro* studies have shown that MEIS1 can also physically interact with HOX proteins (HOXA9) by forming heterodimeric-binding complexes on a DNA target containing a MEIS1 site and an AbdB-like HOX site (Shen *et al*, 1997). MEIS proteins are also major *in vivo* DNA-binding partners for PBX proteins (Chang *et al*, 1997) and can form heterotrimeric complexes with PBX and HOX (Jacobs *et al*, 1999; Shanmugam *et al*, 1999; Shen *et al*, 1999; Schnabel *et al*, 2000). The basis for cooperation between MEIS1 and HOX is therefore likely to be complicated and possibly mediated by heterotrimers, heterodimers, and/or homodimers involving these different proteins.

The ortholog of *Meis1* in *Drosophila* is encoded at the *homothorax* (*hth*) locus (Rieckhof *et al*, 1997; Pai *et al*, 1998). HTH acts upstream of extradenticle (EXD), which is the *Drosophila* ortholog of PBX, and is required for the nuclear localization of EXD. In *Drosophila*, many functions have been ascribed to HTH and EXD, including the regulation of eye development (Pai *et al*, 1998), patterning the embryonic peripheral nervous system (Kurant *et al*, 1998), and proximal–distal limb development (Mercader *et al*, 1999).

*Corresponding author. Center for Cancer Research, Mouse Cancer Genetics Program, National Cancer Institute, Frederick, MD 21702-1201, USA. Tel.: +1 301 846 1260; Fax: +1 301 846 6666;
E-mail: copeland@ncifcrf.gov
[5]These authors contributed equally to this work
[6]Present address: Department of Obstetrics and Gynecology, Osaka University Medical School, Osaka, Japan

Received: 10 June 2003; accepted: 20 November 2003; Published online: 8 January 2004

While homeobox genes were first recognized for their role in pattern formation, it has become increasingly clear in recent years that homeobox genes also have important functions in hematopoiesis (reviewed by, Chiba, 1998). Given MEIS1's role as a HOX and PBX DNA-binding cofactor and its involvement in leukemogenesis, it would not be surprising if MEIS1 were also required for normal hematopoiesis. Here we confirm this prediction and show that mice carrying a germline mutation in *Meis1* have multiple hematopoietic defects. We also show that *Meis1* is required for the development of the microvasculature and the mammalian eye, a role consistent with a recent report suggesting that MEIS1 regulates *Pax6* expression during vertebrate lens development (Zhang *et al*, 2002).

Results

Targeted disruption of Meis1

The *Meis1* knockout mutation was made by replacing part of the homeodomain (exon 8) with a pSAβgeo gene trap cassette (Figure 1A). pSAβgeo contains a splice acceptor site followed by stop codons in all three reading frames, a β-galactosidase-neomycin fusion gene initiated from an internal AUG, and a bovine growth hormone polyadenylation signal sequence (Friedrich and Soriano, 1991). βgeo will therefore be transcribed from the *Meis1* promoter in mutant animals. Male chimeras carrying this mutation were mated to C57BL6/NCr (B6) females to generate a mixed B6;129 line and to 129S3/SvImJ females to produce a 129 line. Subsequent intercrosses of heterozygous mutant animals failed to produce any homozygous mutant pups in 297 B6;129 heterozygous intercross progeny or in 239 heterozygous 129 intercross progeny, indicating that *Meis1* is required for embryonic development. Viable *Meis1*$^{-/-}$ B6;129 embryos were observed as late as 14.5 days post-coitus (dpc) (Table I, Figure 1B), although after 13.5 dpc many of the embryos were pale and exhibited hemorrhaging (see below). *Meis1*$^{-/-}$ 129 embryos were not identified after 12.5 dpc, although they had similar hemorrhages. B6 and 129 animals therefore differ in one or more genetic modifiers of *Meis1*. In subsequent experiments only animals from the B6;129 background were used due to the early embryonic death of *Meis1*$^{-/-}$ 129 embryos.

As expected, RT–PCR analysis showed that *Meis1* exons 1–7 are fused to pSAβgeo sequences in the mutant embryos (data not shown). In contrast, no amplification products were detected when primers from exons 7 and 9 were used for amplification, indicating that all *Meis1* transcripts terminate in pSAβgeo sequences. Western blot analysis of wild-type

Table I *Meis1* mutation is embryonic lethal

	+/+	+/−	Alive −/−	Dead
B6;129 Meis1$^{-/-}$ *intercross progeny*				
dpc 10.5	7	7	3	0
dpc 11.5	3	21	6	3
dpc 12.5	5	13	5	1
dpc 13.5	47	71	24	6
dpc 14.5	4	21	6	2
129 Meis1$^{-/-}$ *intercross progeny*				
dpc 10.5	2	12	3	2
dpc 11.5	1	3	3	3
dpc 12.5	23	31	9	10
dpc 13.5	8	21	0	21
dpc 14.5	4	12	0	5

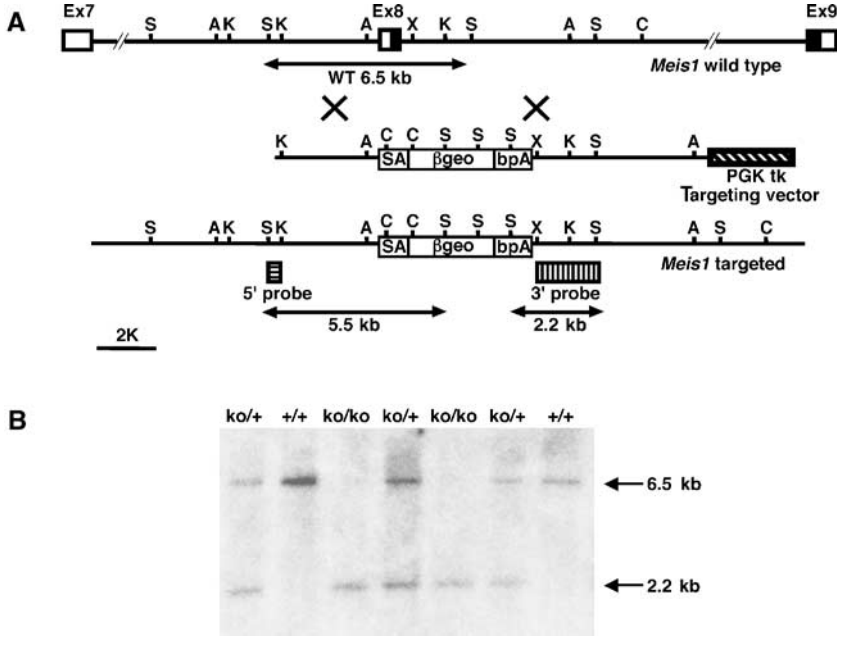

Figure 1 *Meis1*-targeting cassette. (**A**) *Meis1* exon 8 was replaced with a pSAβgeo gene trap targeting cassette. The targeting cassette also contains a thymidine kinase gene driven by a PGK promoter for the negative selection of incorrectly targeted ES cells. Homeodomains located in exons 8 and 9 are represented by black boxes. The 5′ and 3′ probes used for Southern blot analysis are indicated as striped boxes; the sizes of *Sac*I-hybridizing fragments are also indicated. Restriction sites in the introns flanking the targeted exons and the diagnostic restriction fragments for homologous recombinants are indicated (A, *Apa*I, C, *Cla*I, K, *Kpn*I, S, *Sac*I, X, *Xho*I). (**B**) Southern blot analysis of yolk sac DNA prepared from E13.5 embryos generated from a B6;129 *Meis1*$^{+/-}$ intercross and digested with *Sac*I. The wild-type *Meis1* allele is 6.5 kb while the mutated allele is 2.2 kb in size.

E13.5 embryos using a MEIS1-specific antibody identified a wild-type 46 kDa MEIS1 protein that was virtually undetectable in mutant embryos. Heterozygous and homozygous mutant embryos also expressed a smaller, fainter 33 kDa MEIS1 protein (Supplementary Figure 1). This protein is approximately the size predicted for a truncated protein produced from exons 1–7. This protein would contain the MEIS-homology (MH) domain, which interacts with PBX. The MH domain alone causes a phenotype when ectopically expressed in flies (Jaw *et al*, 2000), and mutational analysis of HTH has demonstrated that truncated forms of the protein lacking the homeodomain retain part of their activity (Kurant *et al*, 2001). It is therefore possible that this truncated MEIS1 protein can act as a dominant negative, or that the null phenotype would be slightly different from what is described here for our mutant animals. No differences, however, between heterozygous and wild-type littermates were detected in any of our studies (see below), suggesting that this protein does not act as a strong dominant negative.

Meis1 expression

By β-galactosidase staining, *lacZ* expression from the *Meis1* promoter (hereafter *Meis1-lacZ*) was detected in specific and discrete locations throughout the embryo in a pattern that changed from embryonic day 11 (E11) to E13 (Figure 2A–D). *Meis1-lacZ* staining was comparable to the pattern observed by *in situ* hybridization using a *Meis1* cDNA probe (not shown), but revealed distinct patterns of expression in small regions of the central nervous system and sensory structures of the head, including the ears, eyes, and nose (Figure 2A and C). In the head, strong staining in the eye (white arrowheads in Figure 2A and C) and external ear primordia (ea in Figure 2C) was visible at E11, as well as a faint band of expression in the cochlear neuroepithelium (arrow in Figure 2E). Other regions of intense staining were the soft tissues of the mediastinum (m) and midgut (mg) (Figure 2A, B and D) and the spinal cord, which displayed several intense longitudinal stripes (black arrows; Figure 2B and D). Internal organs with strong expression included all four cardiac chambers and the lungs. This pattern was recapitulated at E13 with some expansion of labeling in the brain. At E13, a thin band of staining in the neuroepithelium of the cochlear canal was also observed (arrow in Figure 2E). By this age, it is apparent that the labeling in the olfactory epithelium occurs transiently in a dorsal to ventral and medial to lateral progression, following the maturational gradient of the olfactory epithelium, with *Meis1-lacZ* expressed in the newest part of the epithelium only (arrows in Figure 2F).

In general, staining in *Meis1*$^{-/-}$ animals was more widespread and intense than in *Meis1*$^{+/-}$ animals, which likely reflects a higher dosage of the reporter gene. However, several striking differences were apparent. At E13, a strong anteroposterior stripe of expression running on the surface of the face from the eye to the nose was found in homozygotes (white asterisks in Figure 2C, F and H) and this expression was completely absent in heterozygotes (Figure 2G). In heterozygotes, *Meis1-lacZ* was also expressed in scattered cells in the liver at both E11 and E13; in homozygotes, expression was observed in only a few cells in the liver at E11 and in no cells at E13. These cells are megakaryocytes, which die in the absence of *Meis1* activity (see below). Strong circumferential expression around the eye field was also observed only in homozygotes (black arrows in Figure 2H and L). By contrast, in heterozygotes, but not in homozygotes, *Meis1-lacZ* was expressed in the posterior lens (arrows in Figure 2K) and surface ectoderm (arrowheads in Figure 2K).

Some structures that reacted positive for β-galactosidase in the *Meis1*$^{-/-}$ embryos retained normal morphology and structure at E13.5. A striking exception was the eye. In homozygotes, the lens was smaller (asterisks in Figure 2J

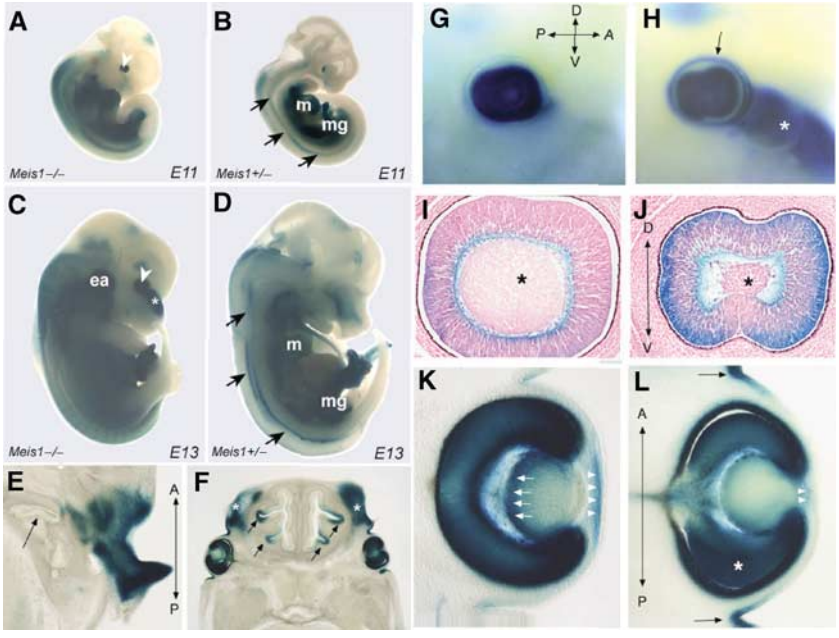

Figure 2 *Meis1* expression revealed by β-galactosidase staining. Whole-mount (**A**, **C**, **G**, **H**), sagittal (**B**, **D**, **I**, **J**), and transverse (**E**, **F**, **K**, **L**) sections of heterozygous *Meis1*$^{+/-}$ (A, C, G, I, K) and homozygous *Meis1*$^{-/-}$ (B, D, E, F, H, J, L) mutant embryos at E11.5 (A, B) and E13.5 (C–L) days of embryonic development stained for *Meis1-lacZ* expression. Anteroposterior (AP) and dorsoventral (DV) axes are marked.

and I), but contact between the lens and surface ectoderm was maintained (white arrowheads in Figure 2L). The retina was also abnormal (compare Figure 2G, I and K to Figure 2H, J and L) and may be partially duplicated, although this possibility will need to be confirmed by additional marker analysis. These abnormalities are not visible at E11 (A) and could only be seen at E13 (Figure 2F, H, J and L). In addition to the eye, abnormalities were also observed in the brain, heart, lungs, and kidneys, among others, suggesting pleiotropic effects of this gene in organogenesis. While the exact nature of these abnormalities remains to be elucidated, the defects in the brain are consistent with the known role of *Meis* genes in patterning of the hindbrain (Dibner *et al*, 2001; Choe *et al*, 2002). By contrast, at this early stage we did not detect any obvious proximal or distal limb defects as has been reported in *Drosophila hth* embryos (Mercader *et al*, 1999). This was surprising, given that MEIS1-related proteins play critical roles in proximodistal axis formation in the limbs of both flies (Wu and Cohen, 1999) and chicken (Mercader *et al*, 1999). The gene is also expressed in the proximal limb buds of mice (Saleh *et al*, 2000) and a *Pbx1* knockout has demonstrated an obligatory role for this gene in patterning of the limbs (Selleri *et al*, 2001).

Megakaryocytes are absent in Meis1$^{-/-}$ *embryos*

Microscopic evaluation revealed extensive hemorrhaging in the brain and trunk of E13.5 *Meis1*$^{-/-}$ embryos, although the extent of hemorrhaging varied among the mutant embryos (Figure 3A). Detailed microscopic analysis of the yolk sac did not reveal significant morphologic differences between mutant and control littermates except for loss of blood within yolk sac blood vessels, and the bleeding seen in *Meis1*$^{-/-}$ embryos appeared to coincide with the time of embryonic death. Because bleeding could result in part (although not exclusively, see below) from megakaryocytes/platelet defects, we stained livers from E13.5 heterozygous and homozygous mutant embryos with hematoxylin and eosin and examined them for megakaryocytes. Megakaryocytes were clearly visible in *Meis1*$^{+/-}$ livers but not in *Meis1*$^{-/-}$ livers (Figure 4A and B). Likewise, β-galactosidase-positive megakaryocytes were seen in *Meis*$^{+/-}$ livers but not in *Meis1*$^{-/-}$ livers (Figure 4C and D). Cells expressing CD41, a megakaryocytic marker (Shattil *et al*, 1985; Gewirtz, 1995), were also absent in the *Meis1*$^{-/-}$ livers (Figure 4E and F). These results show that *Meis1* is expressed in megakaryocytes and is essential for their development.

To confirm these observations, we cultured E13.5 fetal liver cells *in vitro* in the presence of thrombopoietin, interleukin-3 (IL-3), and IL-6. These culture conditions stimulate hematopoietic megakaryocytic progenitors, colony-forming units-megakaryocytes (CFU-Meg), to grow *in vitro* (Kaushansky, 1995; Broudy and Kaushansky, 1998). After 6–8 days, cultures were stained for acetylcholinesterase activity and the number of acetylcholinesterase-positive CFU-Meg scored. In one experiment, an average of 7.2 ± 2.4 CFU-Meg colonies was scored in cultures derived from 5×10^4 wild-type fetal liver cells ($n = 4$), while a similar number of CFU-Meg colonies (6.3 ± 3.4) were scored in *Meis1*$^{+/-}$ cultures ($n = 4$). In contrast, no CFU-Meg colonies were detected in cultures

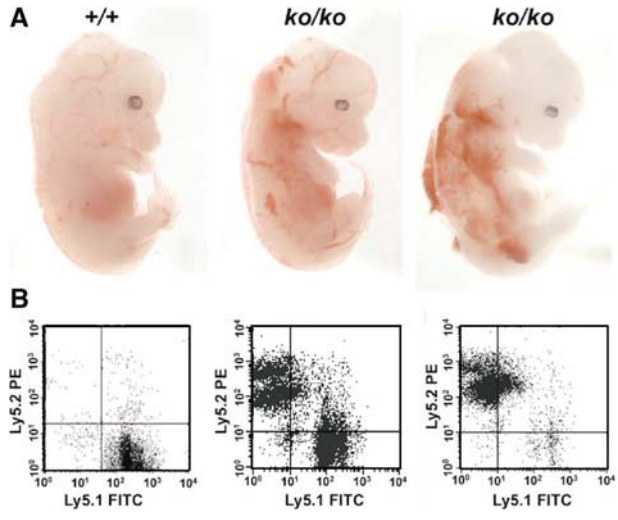

Figure 3 Phenotype of *Meis1* mutant embryos and transplant recipients. (**A**) A wild-type E13.5 and two *Meis1*$^{-/-}$ mutant B6;129 littermates. At this stage, most *Meis1*$^{-/-}$ embryos exhibited hemorrhaging in the brain and trunk. The level of hemorrhaging varied between mutant embryos, with most embryos showing the very extensive hemorrhaging seen in the embryo on the right. (**B**) FACS analysis of bone marrow cells 130 days or more after transplantation of 2×10^6 *Ly5.1*$^+$ fetal liver cells derived from the embryos shown in (A) mixed with 5×10^5 wild-type C57BL/6-*Ly5.2*$^+$ adult bone marrow cells transplanted to lethally irradiated C57BL/6-*Ly5.2*$^+$ hosts. Transplant recipients were stained with FITC-labeled antibodies directed against *Ly5.1*$^+$ or *Ly5.2*$^+$ cells to discriminate between donor and host hematopoietic cells.

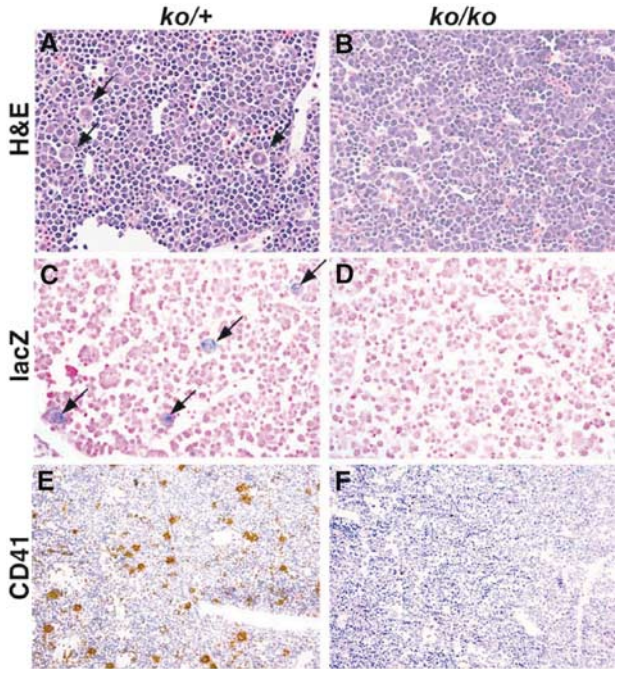

Figure 4 Megakaryocyte defects in *Meis1* mutant embryos. Hematoxylin and eosin staining of paraffin sections through the liver of E13.5 *Meis1*$^{+/-}$ or *Meis1*$^{+/+}$ embryos (**A**, **C**, **E**) compared to *Meis1*$^{-/-}$ (**B**, **D**, **F**) embryos show large cells consistent with megakaryocytes in *Meis1*$^{+/-}$ and *Meis1*$^{+/+}$ embryos (arrows in (A)). These cells are completely missing in *Meis1*$^{-/-}$ embryos by E11 (B). Likewise, β-galactosidase staining was found in a subpopulation of large liver cells (i.e., megakaryocytes) in *Meis1*$^{+/-}$ embryos (arrows in (C)), but this cell population was absent in *Meis1*$^{-/-}$ embryos (D). Immunoreactivity for CD41, a megakaryocyte marker (Gewirtz, 1995; Shattil *et al*, 1985), normally present on a subset of liver cells at E13.5 (brown spots in (E)), was also lacking in *Meis1*$^{-/-}$ embryos (F).

derived from *Meis1*$^{-/-}$ embryos ($n=4$, data not shown). Similar results were observed in two other experiments.

Recent studies have shown that MEIS1/PBX complexes can synergistically transactivate the platelet factor 4 (*Pf4*) gene in combination with GATA1 and ETS1 (Okada *et al*, 2003). *Pf4* is a lineage specific marker that appears during late stages of megakaryocytic differentiation (Breton-Gorius and Vainchenker, 1986). Retinoic acid, an upstream activator of *Meis1* in vertebrate limb development, also stimulates megakaryocytopoiesis in the presence of thrombopoietin or IL-3 and GM-CSF (Visani *et al*, 1999). These results raise the possibility that MEIS1 may be a master regulator of megakaryocytic gene expression.

Myeloerythroid colony-forming cells are reduced in Meis1$^{-/-}$ *fetal livers*

To determine whether other hematopoietic lineages are affected in *Meis1*$^{-/-}$ mutant embryos, 2×10^4 fetal liver cells from E13.5 embryos were grown in methylcellulose for 6–8 days in SCF, GM-CSF, G-CSF, and EPO and the colonies were scored by morphological criteria for BFU-E, CFU-E, GM-CFU, and CFU-mix colonies. Two-tailed *t*-tests of the total cellularity of the *Meis1*$^{-/-}$ fetal livers ($4.3\times10^6\pm3.1\times10^5$, $n=40$ livers) (mean and standard error) showed a decrease ($P<0.001$, $t=6.361$, 68 degrees of freedom) compared to wild-type ($7.5\times10^6\pm4.1\times10^5$, $n=30$ livers) or *Meis1*$^{+/-}$ ($5.9\times10^6\pm3.3\times10^5$, $n=61$) ($P=0008$, $t=3.472$, 99 degrees of freedom) fetal livers. The total number of colony-forming units per liver in *Meis1*$^{-/-}$ embryos also showed a two- to five-fold reduction compared to wild-type livers (Figure 5). CFU-mix colonies were most affected (five-fold), while the least affected were GM-CFU colonies (two-fold). The hematopoietic defects in *Meis1*$^{-/-}$ embryos are therefore not limited to megakaryocytes.

Meis1$^{-/-}$ *fetal liver cells compete poorly in reconstitution assays*

To determine whether *Meis1*$^{-/-}$ fetal liver cells can reconstitute the hematopoietic system of lethally irradiated mice, 2×10^6 fetal liver cells from E13.5 embryos were transferred

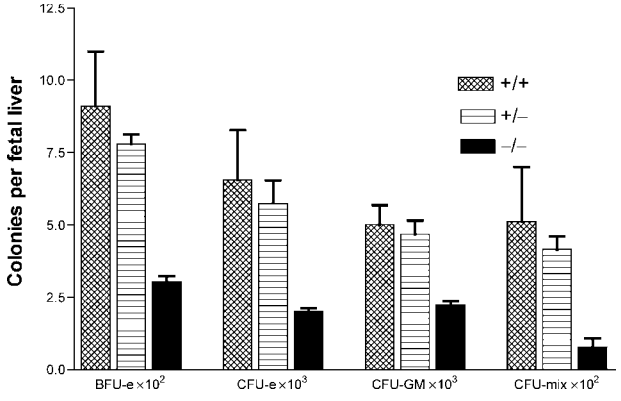

Figure 5 Myeloerythroid colony-forming cells are reduced in *Meis1*$^{-/-}$ fetal livers. Fetal liver cells were isolated from E13.5 wild-type and *Meis1* mutant embryos and scored for the presence of myeloerythroid colony-forming cells. The data shown represent the means and standard deviations from duplicate platings of wild-type ($n=3$, crosshatched bars), *Meis1*$^{+/-}$ ($n=5$, horizontally hatched bars) and *Meis1*$^{-/-}$ ($n=2$, solid bars) fetal livers, and are representative of two separate experiments.

to lethally irradiated hosts. All mice receiving *Meis1*$^{-/-}$ cells ($n=5$) died within 10 days post-transplantation, while mice receiving wild-type ($n=4$) or *Meis1*$^{+/-}$ ($n=7$) cells survived for 40 days (data not shown). *Meis1*$^{-/-}$ fetal liver cells are therefore unable to radioprotect lethally irradiated mice. These data are consistent with the decrease in myeloerythroid colony-forming cells observed *in vitro* in *Meis1*$^{-/-}$ fetal livers.

To determine whether definitive pluripotent hematopoietic progenitors are functionally impaired in *Meis1*$^{-/-}$ embryos, 2×10^6 fetal liver cells from E13.5 mutant embryos were mixed with 5×10^5 wild-type C57BL/6NCr-*Ly5.2*$^+$ adult bone marrow cells and injected into lethally irradiated C57BL/6NCr-*Ly5.2*$^+$ hosts. *Meis1* mutant embryos are *Ly5.1*$^+$, and this cell surface marker can therefore be used to follow the presence of *Meis1* mutant cells in the transplanted hosts. All mice receiving a mixture of mutant and wild-type cells survived 130 days post-transplant, with the exception of one animal that died from causes unrelated to the transplant (data not shown). Mutant *Ly5.1*$^+$ hematopoietic cells in long-term reconstituted recipients were then scored by FACS analysis. The bone marrow of mice transplanted with *Meis1*$^{-/-}$ cells contained $18.1\pm7.7\%$ *Ly5.1*$^+$ cells compared to 85.3 ± 5.2 or $85.9\pm2.2\%$ *Ly5.1*$^+$ cells in recipients receiving *Meis1*$^{+/+}$ or *Meis1*$^{+/-}$ cells, respectively (Figure 6). There was some variability in engraftment, however, as three of the recipients receiving *Meis1*$^{-/-}$ cells showed 30, 48, and 72% engraftment of *Ly5.1*$^+$ cells. These transplant recipients were invariably engrafted with cells taken from embryos that had reduced hemorrhaging (Figure 3B). These embryos may carry one or more *Meis1* modifier genes that protect them from the effects of *Meis1* loss or, alternatively, are slightly delayed in their development compared to *Meis1*$^{-/-}$ embryos with more extensive bleeding, and thus have more *Ly5.1*$^+$ hematopoietic stem cells (HSCs) that can repopulate the hematopoietic system of irradiated hosts.

The level of engraftment in the spleen was similar to that observed in bone marrow. In the spleen, $18.2\pm3.3\%$ of the cells in mice receiving *Meis1*$^{-/-}$ cells were *Ly5.1*$^+$ compared to 86.0 ± 3.2 or $82.9\pm2.7\%$ in recipients receiving *Meis1*$^{+/+}$ or *Meis1*$^{+/-}$ cells, respectively (Figure 6). In the thymus, $4.1\pm1.9\%$ of the cells in mice receiving *Meis1*$^{-/-}$ cells were *Ly5.1*$^+$ compared to 93.6 ± 0.3 or $79.9\pm5.2\%$ in recipients receiving *Meis1*$^{+/+}$ or *Meis1*$^{+/-}$ cells, respectively (Figure 6). In the three mice showing $>30\%$ engraftment of *Meis1*$^{-/-}$ cells in the bone marrow, increased engraftment of *Meis1*$^{-/-}$ cells was also seen in the spleen of all mice (25, 25, 29%) and the thymus of one mouse (21%).

The bone marrow, spleen, and thymus of mice showing $>30\%$ engraftment in the bone marrow were further analyzed for the presence of *Ly5.1*$^+$ cells expressing cell surface markers characteristic of primitive progenitors (CD117, CD34) or more committed lineage-restricted cells (Mac-1, Gr-1, CD61, Ter119, B220, CD3, DX5) (data not shown). These studies showed that *Meis1*$^{-/-}$ cells are capable of differentiating into granulocytes, neutrophils, erythrocytes, B- and T-cells, and NK cells in transplanted hosts, although the overall level of engraftment of each cell type was severely reduced compared to animals transplanted with *Meis1*$^{+/+}$ or *Meis1*$^{+/-}$ cells.

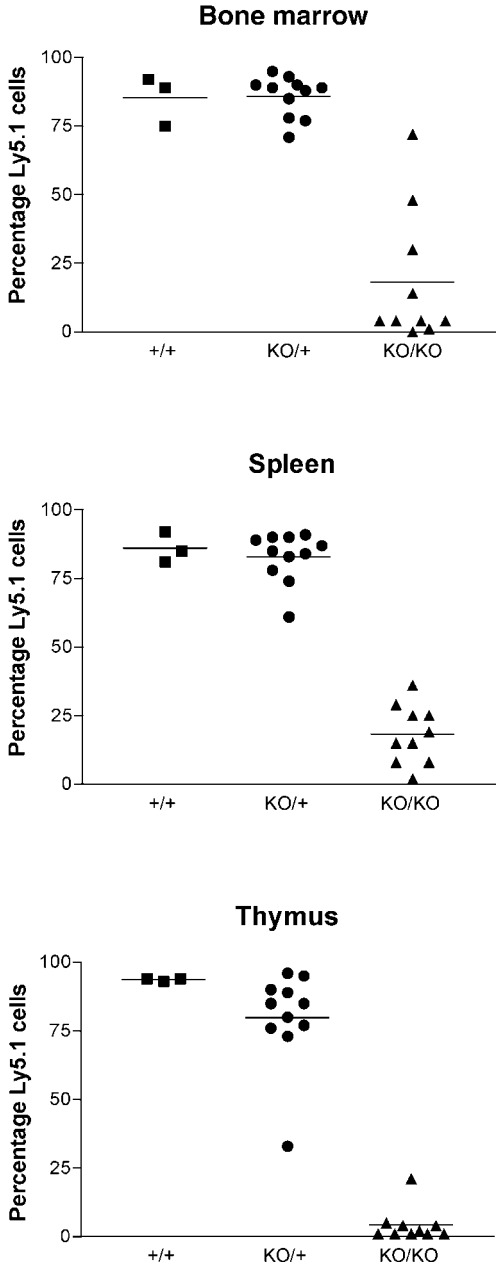

Figure 6 *Meis1* mutant fetal liver cells compete poorly in hematopoietic reconstitution assays. Two million fetal liver cells isolated from E13.5 embryos produced from an N7 C57BL/6-*Ly5.1*$^{+}$ *Meis1*$^{+/-}$ intercross plus 4×10^5 adult bone marrow cells from C57BL/6-*Ly5.2*$^{+}$ mice were transplanted to irradiated C57BL/6-*Ly5.2*$^{+}$ hosts. The genotype of each embryo was determined by Southern blot analysis of yolk sac DNA. At 130 days or greater after transplantation, recipients of fetal liver cells from wild-type (closed squares, $n = 3$), *Meis1*$^{+/-}$ (closed circles, $n = 11$), or *Meis1*$^{-/-}$ embryos (closed triangles, $n = 10$) were analyzed for donor engraftment (*Ly5.1*$^{+}$ cells) in the bone marrow, spleen, and thymus by flow cytometry. A horizontal line indicates the mean level of engraftment.

Defective angiogenesis in Meis1$^{-/-}$ *embryos*

Although *Meis1*$^{-/-}$ embryos fail to make megakaryocytes/platelets, it is unlikely that this alone causes the hemorrhaging seen in *Meis1*$^{-/-}$ embryos since *Nfe2*$^{-/-}$ mutant embryos, which have platelet defects due to a block in megakaryocyte maturation (Shivdasani *et al*, 1995), are born in normal numbers and do not hemorrhage *in utero*. To determine whether hemorrhaging in *Meis1*$^{-/-}$ mutant embryos could result from defects in vasculogenesis (the differentiation of mesodermally derived endothelial cell precursors into vascular channels) or angiogenesis, (the formation of smaller vessels and the microvasculature), we evaluated the large blood vessels and microvasculature in *Meis1*$^{-/-}$ mutant embryos and control littermates at E13.5 (Figure 7). In *Meis1*$^{-/-}$ embryos, expressions of α-smooth muscle actin (SMA) and PECAM (CD31), a marker for endothelial cells, were abnormal. Unlike normal embryos, where antibodies to these molecules outline branching capillaries with a clear lumen and consistent size (Figure 7A and C), in mutant embryos these markers were found together in close association but failed to delineate a clear lumen (Figure 7B and D). Moreover, the branching pattern and size of the vessels was abnormal. In normal embryos the capillaries were just large enough to enclose red blood cells (RBCs) (Figure 7C), while in *Meis1*$^{-/-}$ embryos the small vessels were either too narrow to admit RBCs (Figure 7B and D) or formed larger sinuses where the RBCs pooled. Numerous extravagated RBCs were also found outside the microvasculature in surrounding tissues in *Meis1*$^{-/-}$ embryos. In contrast, the major blood vessels were normal in *Meis1*$^{-/-}$ embryos (Figure 7E and F).

To determine whether the capillary defects observed in *Meis1*$^{-/-}$ embryos are cell autonomous or cell non-autonomous, we stained tissue sections of E13.5 wild-type embryos with antibodies to MEIS1 and PECAM or SMA, markers of vascular endothelium and vascular smooth muscle, respectively. While we sometimes observed MEIS1 expression in the vicinity of PECAM and SMA, we did not see a direct correlation between the sites of MEIS1 and PECAM and SMA expression (Figure 7G–I). Moreover, PECAM-1 and SMA were often found in regions that lacked MEIS1 expression and vice versa. We also observed individual *Meis1-lacZ*-positive cells in regions of hemorrhage in the dorsal flanks of *Meis1*$^{-/-}$ embryos, but not in a pattern suggestive of capillaries (data not shown). In addition, in no region could we detect *Meis1-lacZ* expression in a blood vessel-specific pattern. Taken together, these results suggest that the angiogenic defects in *Meis1*$^{-/-}$ embryos are cell nonautonomous with respect to MEIS1 expression, although conditional gene knockouts will be required to confirm these results.

Discussion

Here we show that *Meis1*, a member of the TALE family of homeobox genes, is required for embryonic viability, eye development, and maintenance of definitive hematopoiesis. *Meis1*-deficient embryos also lack megakaryocytes, display extensive hemorrhaging in the brain and trunk, and have defects in angiogenesis. The eye defects observed in *Meis1*$^{-/-}$ embryos are consistent with recent studies suggesting that *Meis1* is a regulator of *Pax6* expression in prospective lens ectoderm (Zhang *et al*, 2002). *Pax6* is a pivotal regulator of eye development throughout Metazoans, but the upstream regulators of *Pax6* have remained elusive. A strong anteroposterior stripe of *Meis1* expression running on the surface of the face from the eye to the nose was also seen in *Meis1*$^{-/-}$ embryos. This expression was absent in *Meis1*$^{+/-}$ embryos. The cause of this ectopic expression remains to be determined, but one possibility is that it represents the presence of

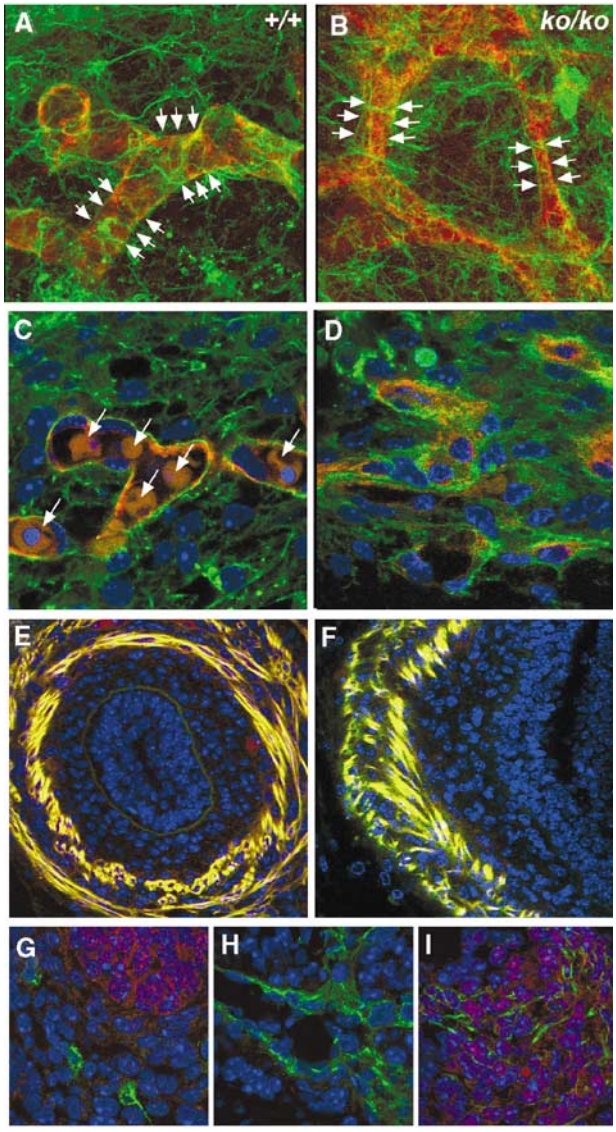

Figure 7 *Meis1* mutant embryos have angiogenesis defects. Confocal images (**A–F**) were acquired of blood vessels identified by PECAM/CD31 (red) and SAM (green) from normal (A, C, E) and *Meis1*$^{-/-}$ mutant (B, D, F) E13.5 embryos. Nuclei are labeled with DAPI (blue). A 15–20 μm stack of images was combined to generate a three-dimensional projection (A, B), showing a branching capillary with clear lumen in the normal (A) but lack of this structure in the mutant (B). Normal capillaries displayed consistent size, while those in the *Meis1*$^{-/-}$ tissue did not (arrows in A, B). In 1 μm confocal images, RBCs normally filled the lumen of capillaries (arrows in C). This feature was lacking in *Meis1*$^{-/-}$ embryos, which formed irregular and disorganized microvasculature (D). The major blood vessels showed exact colocalization of PECAM (red) and SMA (green), resulting in a yellow signal (E, F). Large blood vessels (e.g. major arteries leaving the thorax) were present in *Meis1*$^{-/-}$ embryos and displayed normal lumen formation (F). Confocal images (**G–I**) of wild-type E13.5 embryo sections stained with antibodies to MEIS1 (red) and either PECAM/CD31 (green, G, H) or SMA (green, I). Nuclei are labeled with DAPI (blue). Various regions of the embryo show MEIS1 and PECAM in close but nonoverlapping proximity (G). Other regions of angiogenesis express PECAM without MEIS1 (H). Yet other areas are positive for both an angiogenic marker (SAM) and MEIS1. Original magnification, 100 ×.

additional eye primordia. Evidence for this hypothesis comes from flies where HTH and EXD function as negative regulators of eye develop and delimit the eye fields (Pai *et al*, 1998).

Defects in primitive hematopoiesis were not observed in *Meis1*$^{-/-}$ embryos. Definitive hematopoiesis is, however, initiated in *Meis1*$^{-/-}$ mutant embryos as evidenced by the colony formation of fetal liver committed progenitors and multilineage reconstitution of irradiated hosts following transplantation of *Meis1*$^{-/-}$mutant fetal liver cells (Palis *et al*, 1999). Compared to wild-type and heterozygous mutant cells, E13.5 *Meis1*$^{-/-}$ cells competed poorly in reconstitution assays, suggesting a possible decrease in the number of HSCs and/or a defect in the proliferation or differentiation of more committed progenitors. *Meis1* appears to act later in embryonic development than other transcription factors such as GATA3 (Pandolfi *et al*, 1995), RUNX1 (Okuda *et al*, 1996; Wang *et al*, 1996a), or CBFB (Wang *et al*, 1996b), which produce more severe defects in definitive hematopoiesis. Hemorrhaging and death in these mutant embryos occurs between 11.5 and 12.5 dpc.

Pbx1 and *Meis1* mutant animals share several phenotypes in common, including defects in definitive hematopoiesis (DiMartino *et al*, 2001). This is interesting since PBX1 is a major *in vivo* DNA-binding partner of MEIS1. Definitive myeloerythroid lineages are present in *Pbx1* and *Meis1* mutant animals, and the number of colony-forming cells is substantially reduced in both (DiMartino *et al*, 2001). *Pbx1*$^{-/-}$ fetal liver cells also perform poorly in competitive repopulation assays, as do *Meis1*$^{-/-}$ fetal liver cells. Both mutants also display defects in kidney development (Schnabel *et al*, 2003 and our unpublished observations). There are some differences, however, in the two mutant phenotypes. *Meis1* mutant animals do not develop the skeletal abnormalities observed in *Pbx1*$^{-/-}$ mice (Selleri *et al*, 2001). They also fail to make megakaryocytes/platelets and they show extensive hemorrhaging, unlike *Pbx1*$^{-/-}$ mutant animals, which make platelets and do not hemorrhage. *Pbx1*$^{-/-}$ embryos die later in development than *Meis1*$^{-/-}$ embryos (15.5–16.5 dpc versus 12.5–14.5 dpc). *Pbx1*$^{-/-}$ fetal liver cells also radioprotect lethally irradiated mice, although they are only half as effective at radioprotection as *Pbx1*$^{+/+}$ cells (Chang *et al*, 1997), in contrast to *Meis1*$^{-/-}$ cells, which are unable to radioprotect lethally irradiated mice. Perhaps other PBX proteins that can interact with MEIS1 provide partial compensation for the loss of *Pbx1* in knockout mice.

Meis1 is expressed at the highest levels in the Sca-1^{+}Lin^{-} fraction of the adult bone marrow and E14.5 fetal liver (Pineault *et al*, 2002). This fraction is highly enriched in HSCs (Rebel *et al*, 1996). In contrast, the expression of *Meis1* in more committed progenitors is barely detectable or undetectable. A close correlation between the onset of *Meis1* expression in embryoid body development and the appearance of hematopoietic cells has also been seen (Pineault *et al*, 2002). Many *Hox* genes are expressed at their highest levels in the Sca1^{+}Lin^{-} fraction and are rapidly downregulated during hematopoietic differentiation (Pineault *et al*, 2002), findings consistent with a major role of MEIS1 in normal hematopoiesis as a HOX cofactor. *Meis1* might therefore be required for the proliferation/self-renewal of the HSC, a hypothesis that is supported by studies presented here and the failure of *Meis1*$^{-/-}$ fetal liver cells to contribute efficiently to multiple hematopoietic lineages in transplanted lethally irradiated recipients.

HSCs produce angiopoeitin (AGPT), a molecule that is critical for angiogenesis (Takakura *et al*, 2000). Embryos

deficient in HSCs (Takakura *et al*, 2000), or that have defects in *Agpt* (Suri *et al*, 1996) or the AGPT receptors *Tie1* and *Tie2* (Puri *et al*, 1995; Sato *et al*, 1995), exhibit microvascularization defects and show extensive hemorrhaging and death between E9.5 and E13.5. These results, and those suggesting that the vascular defects in *Meis1*$^{-/-}$ embryos are cell non-autonomous with respect to MEIS1 expression, provide further evidence for an HSC defect in *Meis1*$^{-/-}$ embryos and suggest that hemorrhaging in *Meis1*$^{-/-}$ animals is due to an HSC defect resulting from a decrease in the secretion of AGPT and the failure to form normal microvascular channels.

Materials and methods

Meis1 mutant animals

Meis1 exon 8 was replaced with a pSAβgeo cassette (Figure 1A). Homologous targeting events were identified by Southern blotting using 0.5 kb *Sac*I-*Kpn*I (5′) or 1.9 kb *Sac*I-*Xho*I (3′) probes (Figure 1A), labeled using a Megaprime DNA kit (Amersham Biosciences, Piscataway, NJ). Several independent ES cell clones carrying the knockout allele were isolated and the mutation was introduced into the germline by standard techniques. Mice were maintained under limited access conditions at the National Cancer Institute (Frederick) and animal care was provided according to the procedures outlined in the Guide for the Care and Use of Laboratory Animals, under an approved animal care and use committee protocol.

Immunohistochemical and confocal analysis

Embryos were collected at 12.5–13.5 dpc with the morning of vaginal plug detection considered as 0.5 dpc. Embryos were dissected from the uterus and fixed in 4% paraformaldehyde in PBS. For some studies, embryos were embedded in paraffin. After dewaxing, sections of embedded embryos were incubated with a rat anti-mouse CD41 antibody (MWReg30, BD Pharmingen, San Diego, CA) followed by a biotinylated antibody directed against rat IgG antibody labeled with the avidin/biotinylated enzyme complex (Vector Laboratories, Burlingame, CA). A signal was detected with 3,3′-diaminobenzidine (Vector Laboratories) as chromogen. For other studies, embryos were embedded in 3% agarose, vibratome-sectioned, and immunostained with DAPI (Molecular Probes, Eugene, OR) and antibodies to PECAM/CD31 (BD Pharmingen, San Diego, CA) and SMA (Dako, Glustrup, Denmark). Secondary antibodies were Cy2- and Cy3-conjugated goat anti-mouse or goat anti-rat IgG (Jackson Immunoresearch, West Grove, PA). Images were acquired on a Zeiss 510 confocal laser-scanning microscope (Carl Zeiss, Germany). For three-dimensional analysis of blood vessels, stacks of images were acquired and converted to a maximum intensity projection.

X-gal staining

Paraformaldehyde-fixed embryos at E11.5 and E13.5 were stained overnight at 37°C in the dark with 1 mg/ml X-gal (US Biological, Swampscott, MA), 4 mM $K_4Fe(CN)_63H_2O$, 4 mM $K_3Fe(CN)_6$, 2 mM $MgCl_2$ in PBS to detect beta-galactosidase (beta-gal) activity.

Myeloerythroid colony assays

Megakaryocyte colony-forming units were assayed by plating 5×10^4 fetal liver cells on chamber culture slides in collagen-based medium (Stem Cell Technologies, Vancouver, BC) containing 50 ng/ml human thrombopoietin (R and D Systems, Minneapolis, MN), 10 ng/ml murine interleukin-3 (IL-3), and 20 ng/ml murine IL-6 (PeproTech, Rocky Hill, NJ). After 6–8 days of incubation, the slides were stained for acetylcholinesterase activity according to the manufacturer's directions and scored for the presence of red-brown to brown-black granules in cells. BFU-e, CFU-e, CFU-GM, and CFU-mix were assayed by plating 2×10^4 fetal liver cells in 35 mm dishes in methylcellulose medium (M3334, Stem Cell Technologies), which contains 3 units/ml of EPO and supplemented with 20 ng/ml SCF, 5 ng/ml murine GM-CSF, and 5 ng/ml murine G-CSF (PeproTech). Dishes were incubated in a humidified 5% CO_2 atmosphere at 37°C and colonies were counted 3–8 days after plating.

Fetal liver transplantation

Eight to twelve week old female C57BL/6-*Ly5.2.* mice were irradiated with 1100 rads from a ^{137}Cs source at a rate of 167 rad per minute. After 4 h, 2×10^6 E13.5 fetal liver cells produced from B6.129 *Meis1*$^{+/-}$ intercrosses were transplanted to irradiated hosts by tail vein injection. In some experiments, $4–5 \times 10^5$ bone marrow cells from 8- to 12-week-old female C57BL/6Ncr-*Ly5.2* mice were injected along with the fetal liver cells. Single-cell suspensions were made from hematopoietic organs of transplant recipients and red cells lysed by incubation in ice-cold ACK lysis buffer (Quality Biological, Gaithersburg, MD) for 10 min. Cells were washed twice in DPBS, 1% fetal calf serum (FCS, Atlanta Biologicals, Norcross, GA) and incubated with 2 μg/10^6 cells rat anti-mouse CD16/CD32 antibody (2.4G2, BD Pharmingen, San Diego, CA) for 30 min on ice, washed twice in DPBS, 1% FCS and incubated for 30 min on ice with fluorescin isothiocyanate (FITC) or phycoerythrin (PE)-conjugated antibodies (BD Pharmingen): 0.5 μg/10^6 cells of rat anti-mouse CD3 (17A2), CD4 (GK1.5), CD8a (53-6.7), CD19 (1D3), CD23 (B3B4), CD25 (PC61), CD34 (RAM34), CD45/B220 (RA3-6B2), CD62P (RB40.34), CD117 (ACK45), Gr-1 (RB6-8C5), Ly-76(Ter119), and isotype controls (R35-95 and MWReg30), 0.125 μg/10^6 cells of rat anti-mouse CD11b (M1/70), and 0.25 μg/10^6 cells mouse anti-mouse CD45.2 (*Ly5.1*, 104) and CD45.1 (*Ly5.2*, A20). Cells were then washed twice in DPBS, 1% FCS, fixed in 1% paraformaldehyde/PBS, and analyzed on a FACS Caliber flow cytometer (Becton Dickinson, San Jose, CA). Percentage engraftment was determined in comparison to isotype control antibodies.

Supplementary data

Supplementary data are available at *The EMBO Journal* Online.

Acknowledgements

We thank Deborah Swing, Holly Morris, and Sandra Grimm for animal handling, Debra Gilbert, Norene O'Sullivan, Deborah Householder, Anna Trivett, and Tukari Yamazaki for technical help, Linda Cleveland for sequencing, Eileen Southon for ES manipulation, Mary Ellen Palko for providing primers, Ed Cho for confocal microscopy assistance, Keith Rogers for pathological advice, Linda Brubaker and Madeline Knoebel for secretarial assistance and Michael Cleary for a critical reading of this manuscript. This research was supported in part by a Grant in Aid for Scientific Research on Priority Area C from the Ministry of Education, Science, Sport and Culture, Japan and the National Cancer Institute, DHHS, USA.

References

Afonja O, Smith Jr JE, Cheng DM, Goldenberg AS, Amorosi E, Shimamoto T, Nakamura S, Ohyashiki K, Ohyashiki J, Toyama K, Takeshita K (2000) MEIS1 and HOXA7 genes in human acute myeloid leukemia. *Leuk Res* **24:** 849–855

Berthelsen J, Viggiano L, Schulz H, Ferretti E, Consalez GG, Rocchi M, Blasi F (1998) PKNOX1, a gene encoding PREP1, a new regulator of Pbx activity, maps on human chromosome 21q22.3 and murine chromosome 17B/C. *Genomics* **47:** 323–324

Borrow J, Shearman AM, Stanton Jr VP, Becher R, Collins T, Williams AJ, Dube I, Katz F, Kwong YL, Morris C, Ohyashiki K, Toyama K, Rowley J, Housman DE (1996) The t(7;11)(p15;p15) translocation in acute myeloid leukaemia fuses the genes for nucleoporin NUP98 and class I homeoprotein HOXA9. *Nat Genet* **12:** 159–167

Breton-Gorius J, Vainchenker W (1986) Expression of platelet proteins during the *in vitro* and *in vivo* differentiation of

megakaryocytes and morphological aspects of their maturation. *Semin Hematol* **23:** 43–67
Broudy VC, Kaushansky K (1998) Biology of thrombopoietin. *Curr Opin Pediatr* **10:** 60–64
Chang CP, Jacobs Y, Nakamura T, Jenkins NA, Copeland NG, Cleary ML (1997) Meis proteins are major *in vivo* DNA binding partners for wild-type but not chimeric Pbx proteins. *Mol Cell Biol* **17:** 5679–5687
Chiba S (1998) Homeobox genes in normal hematopoiesis and leukemogenesis. *Int J Hematol* **68:** 343–353
Choe SK, Vlachakis N, Sagerstrom CG (2002) Meis family proteins are required for hindbrain development in the zebrafish. *Development* **129:** 585–595
Dibner C, Elias S, Frank D (2001) XMeis3 protein activity is required for proper hindbrain patterning in Xenopus laevis embryos. *Development* **128:** 3415–3426
DiMartino JF, Selleri L, Traver D, Firpo MT, Rhee J, Warnke R, O'Gorman S, Weissman IL, Cleary ML (2001) The Hox cofactor and proto-oncogene Pbx1 is required for maintenance of definitive hematopoiesis in the fetal liver. *Blood* **98:** 618–626
Friedrich G, Soriano P (1991) Promoter traps in embryonic stem cells: a genetic screen to identify and mutate developmental genes in mice. *Genes Dev* **5:** 1513–1523
Gewirtz AM (1995) Megakaryocytopoiesis: the state of the art. *Thromb Haemost* **74:** 204–209
Jacobs Y, Schnabel CA, Cleary ML (1999) Trimeric association of Hox and TALE homeodomain proteins mediates Hoxb2 hindbrain enhancer activity. *Mol Cell Biol* **19:** 5134–5142
Jaw TJ, You LR, Knoepfler PS, Yao LC, Pai CY, Tang CY, Chang LP, Berthelsen J, Blasi F, Kamps MP, Sun YH (2000) Direct interaction of two homeoproteins, homothorax and extradenticle, is essential for EXD nuclear localization and function. *Mech Dev* **91:** 279–291
Kamps MP, Murre C, Sun XH, Baltimore D (1990) A new homeobox gene contributes the DNA binding domain of the t(1;19) translocation protein in pre-B ALL. *Cell* **60:** 547–555
Kaushansky K (1995) Thrombopoietin: the primary regulator of platelet production. *Blood* **86:** 419–431
Kroon E, Krosl J, Thorsteinsdottir U, Baban S, Buchberg AM, Sauvageau G (1998) Hoxa9 transforms primary bone marrow cells through specific collaboration with Meis1a but not Pbx1b. *EMBO J* **17:** 3714–3725
Kurant E, Eytan D, Salzberg A (2001) Mutational analysis of the Drosophila homothorax gene. *Genetics* **157:** 689–698
Kurant E, Pai CY, Sharf R, Halachmi N, Sun YH, Salzberg A (1998) Dorsotonals/homothorax, the Drosophila homologue of meis1, interacts with extradenticle in patterning of the embryonic PNS. *Development* **125:** 1037–1048
Lawrence HJ, Rozenfeld S, Cruz C, Matsukuma K, Kwong A, Komuves L, Buchberg AM, Largman C (1999) Frequent co-expression of the HOXA9 and MEIS1 homeobox genes in human myeloid leukemias. *Leukemia* **13:** 1993–1999
Mercader N, Leonardo E, Azpiazu N, Serrano A, Morata G, Martinez C, Torres M (1999) Conserved regulation of proximodistal limb axis development by Meis1/Hth. *Nature* **402:** 425–429
Monica K, Galili N, Nourse J, Saltman D, Cleary ML (1991) PBX2 and PBX3, new homeobox genes with extensive homology to the human proto-oncogene PBX1. *Mol Cell Biol* **11:** 6149–6157
Moskow JJ, Bullrich F, Huebner K, Daar IO, Buchberg AM (1995) Meis1, a PBX1-related homeobox gene involved in myeloid leukemia in BXH-2 mice. *Mol Cell Biol* **15:** 5434–5443
Nakamura T, Jenkins NA, Copeland NG (1996a) Identification of a new family of Pbx-related homeobox genes. *Oncogene* **13:** 2235–2242
Nakamura T, Largaespada DA, Lee MP, Johnson LA, Ohyashiki K, Toyama K, Chen SJ, Willman CL, Chen IM, Feinberg AP, Jenkins NA, Copeland NG, Shaughnessy Jr JD (1996b) Fusion of the nucleoporin gene NUP98 to HOXA9 by the chromosome translocation t(7;11)(p15;p15) in human myeloid leukaemia. *Nat Genet* **12:** 154–158
Nakamura T, Largaespada DA, Shaughnessy JD, Jr, Jenkins NA, Copeland NG (1996c) Cooperative activation of Hoxa and Pbx1-related genes in murine myeloid leukaemias. *Nat Genet* **12:** 149–153
Nourse J, Mellentin JD, Galili N, Wilkinson J, Stanbridge E, Smith SD, Cleary ML (1990) Chromosomal translocation t(1;19) results in synthesis of a homeobox fusion mRNA that codes for a potential chimeric transcription factor. *Cell* **60:** 535–545
Okada Y, Nagai R, Sato T, Matsuura E, Minami T, Morita I, Doi T (2003) The homeodomain proteins, MEIS1 and PBXs, regulate the lineage specific transcription of the platelet factor 4 gene. *Blood* **101:** 4748–4756
Okuda T, van Deursen J, Hiebert SW, Grosveld G, Downing JR (1996) AML1, the target of multiple chromosomal translocations in human leukemia, is essential for normal fetal liver hematopoiesis. *Cell* **84:** 321–330
Pai CY, Kuo TS, Jaw TJ, Kurant E, Chen CT, Bessarab DA, Salzberg A, Sun YH (1998) The homothorax homeoprotein activates the nuclear localization of another homeoprotein, extradenticle, and suppresses eye development in Drosophila. *Genes Dev* **12:** 435–446
Palis J, Robertson S, Kennedy M, Wall C, Keller G (1999) Development of erythroid and myeloid progenitors in the yolk sac and embryo proper of the mouse. *Development* **126:** 5073–5084
Pandolfi PP, Roth ME, Karis A, Leonard MW, Dzierzak E, Grosveld FG, Engel JD, Lindenbaum MH (1995) Targeted disruption of the GATA3 gene causes severe abnormalities in the nervous system and in fetal liver haematopoiesis. *Nat Genet* **11:** 40–44
Pineault N, Helgason CD, Lawrence HJ, Humphries RK (2002) Differential expression of Hox, Meis1, and Pbx1 genes in primitive cells throughout murine hematopoietic ontogeny. *Exp Hematol* **30:** 49–57
Puri MC, Rossant J, Alitalo K, Bernstein A, Partanen J (1995) The receptor tyrosine kinase TIE is required for integrity and survival of vascular endothelial cells. *EMBO J* **14:** 5884–5891
Rebel VI, Miller CL, Eaves CJ, Lansdorp PM (1996) The repopulation potential of fetal liver hematopoietic stem cells in mice exceeds that of their liver adult bone marrow counterparts. *Blood* **87:** 3500–3507
Rieckhof GE, Casares F, Ryoo HD, Abu-Shaar M, Mann RS (1997) Nuclear translocation of extradenticle requires homothorax, which encodes an extradenticle-related homeodomain protein. *Cell* **91:** 171–183
Rozovskaia T, Feinstein E, Mor O, Foa R, Blechman J, Nakamura T, Croce CM, Cimino G, Canaani E (2001) Upregulation of Meis1 and HoxA9 in acute lymphocytic leukemias with the t(4:11) abnormality. *Oncogene* **20:** 874–878
Saleh M, Huang H, Green NC, Featherstone MS (2000) A conformational change in PBX1A is necessary for its nuclear localization. *Exp Cell Res* **260:** 105–115
Sato TN, Tozawa Y, Deutsch U, Wolburg-Buchholz K, Fujiwara Y, Gendron-Maguire M, Gridley T, Wolburg H, Risau W, Qin Y (1995) Distinct roles of the receptor tyrosine kinases Tie-1 and Tie-2 in blood vessel formation. *Nature* **376:** 70–74
Schnabel CA, Jacobs Y, Cleary ML (2000) HoxA9-mediated immortalization of myeloid progenitors requires functional interactions with TALE cofactors Pbx and Meis. *Oncogene* **19:** 608–616
Schnabel CA, Godin RE, Cleary ML (2003) Pbx1 regulates nephrogenesis and ureteric branching in the developing kidney. *Dev Biol* **254:** 262–276
Selleri L, Depew MJ, Jacobs Y, Chanda SK, Tsang KY, Cheah KS, Rubenstein JL, O'Gorman S, Cleary ML (2001) Requirement for Pbx1 in skeletal patterning and programming chondrocyte proliferation and differentiation. *Development* **128:** 3543–3557
Shanmugam K, Green NC, Rambaldi I, Saragovi HU, Featherstone MS (1999) PBX and MEIS as non-DNA-binding partners in trimeric complexes with HOX proteins. *Mol Cell Biol* **19:** 7577–7588
Shattil SJ, Hoxie JA, Cunningham M, Brass LF (1985) Changes in the platelet membrane glycoprotein IIb.IIIa complex during platelet activation. *J Biol Chem* **260:** 11107–11114
Shen WF, Montgomery JC, Rozenfeld S, Moskow JJ, Lawrence HJ, Buchberg AM, Largman C (1997) AbdB-like Hox proteins stabilize DNA binding by the Meis1 homeodomain proteins. *Mol Cell Biol* **17:** 6448–6458
Shen WF, Rozenfeld S, Kwong A, Kom ves LG, Lawrence HJ, Largman C (1999) HOXA9 forms triple complexes with PBX2 and MEIS1 in myeloid cells. *Mol Cell Biol* **19:** 3051–3061
Shivdasani RA, Rosenblatt MF, Zucker-Franklin D, Jackson CW, Hunt P, Saris CJ, Orkin SH (1995) Transcription factor NF-E2 is required for platelet formation independent of the actions of

thrombopoietin/MGDF in megakaryocyte development. *Cell* **81:** 695–704

Suri C, Jones PF, Patan S, Bartunkova S, Maisonpierre PC, Davis S, Sato TN, Yancopoulos GD (1996) Requisite role of antiopoietin-1, a ligand for the TIE2 receptor, during embryonic angiogenesis. *Cell* **87:** 1171–1180

Takakura N, Watanabe T, Suenobu S, Yamada Y, Noda T, Ito Y, Satake M, Suda T (2000) A role for hematopoietic stem cells in promoting angiogenesis. *Cell* **102:** 199–209

Thorsteinsdottir U, Kroon E, Jerome L, Blasi F, Sauvageau G (2001) Defining roles for HOX and MEIS1 genes in induction of acute myeloid leukemia. *Mol Cell Biol* **21:** 224–234

Visani G, Ottaviani E, Zauli G, Tosi P, Pellacani A, Isidori A, Pierpaoli S, Tura S (1999) All-*trans* retinoic acid at low concentration directly stimulates normal adult megakaryocytopoiesis in the presence of thrombopoietin or combined cytokines. *Eur J Haematol* **63:** 149–153

Wagner K, Mincheva A, Korn B, Lichter P, Popperl H (2001) Pbx4, a new Pbx family member on mouse chromosome 8, is expressed during spermatogenesis. *Mech Dev* **103:** 127–131

Wang Q, Stacy T, Binder M, Marin-Padilla M, Sharpe AH, Speck NA (1996a) Disruption of the Cbfa2 gene causes necrosis and hemorrhaging in the central nervous system and blocks definitive hematopoiesis. *Proc Natl Acad Sci USA* **93:** 3444–3449

Wang Q, Stacy T, Miller JD, Lewis AF, Gu TL, Huang X, Bushweller JH, Bories JC, Alt FW, Ryan G, Liu PP, Wynshaw-Boris A, Binder M, Marin-Padilla M, Sharpe AH, Speck NA (1996b) The CBFbeta subunit is essential for CBFalpha2 (AML1) function *in vivo*. *Cell* **87:** 697–708

Wu J, Cohen SM (1999) Proximodistal axis formation in the Drosophila leg: subdivision into proximal and distal domains by homothorax and distal-less. *Development* **126:** 109–117

Zhang X, Friedman A, Heaney S, Purcell P, Maas RL (2002) Meis homeoproteins directly regulate Pax6 during vertebrate lens morphogenesis. *Genes Dev* **16:** 2097–2107